Splice variants of protein disulfide isomerase - identification, distribution and functional characterization in the rat

Thomas Chetot, Xavier Serfaty, Léna Carret, Alexandre Kriznik, Sophie Rahuel-Clermont, Lucie Grand, Maïwenn Jacolot, Florence Popowycz, Etienne Benoit, Véronique Lambert, et al.

Splice variants of protein disulfide isomerase - identification, distribution and functional characterization in the rat

Thomas Chetot[1], Xavier Serfaty[1], Léna Carret[1], Alexandre Kriznik[2], Sophie-Rahuel-Clermont[2], Lucie Grand[3], Maïwenn Jacolot[3], Florence Popowycz[3], Etienne Benoit[1], Véronique Lambert[1] and Virginie Lattard[1]

[1]USC 1233 RS2GP, VetAgro Sup, INRA, Université de Lyon, 69280, Marcy l'étoile, France

[2]Université de Lorraine, CNRS, IMoPA, F-54000 Nancy, France

[3]Univ Lyon, INSA Lyon, Université Lyon 1, CNRS, CPE Lyon, UMR 5246, ICBMS 69621 Villeurbanne Cedex, France

Corresponding author: Virginie Lattard

virginie.lattard@vetagro-sup.fr

Abstract

Background: Protein Disulfide Isomerase (PDI) enzyme is an emerging therapeutic target in oncology and hematology. Although PDI reductase activity has been studied with isolated fragments of the protein, natural structural variations affecting reductase activity have not been addressed.

Methods: In this study, we discovered four coding splice variants of the *Pdi* pre-mRNA in rats. In vitro Michaelis constants and apparent maximum steady-state rate constants after purification and distribution in different rat tissues were determined.

Results: The consensus sequence was found to be the most expressed splice variant while the second most expressed variant represents 15 to 35 % of total *Pdi* mRNA.

The third variant shows a quasi-null expression profile and the fourth was not quantifiable. The consensus sequence splice variant and the second splice variant are widely expressed (transcription level) in the liver and even more present in males. Measurements of the reductase activity of recombinant PDI indicate that the consensus sequence and third splice variant are fully active variants. The second most expressed variant, differing by a lack of signal peptide, was found active but less than the consensus sequence.

General significance: Our work emphasizes the importance of taking splice variants into account when studying PDI-like proteins to understand the full biological functionalities of PDI.

Keywords

Protein disulfide isomerase (PDI), Splice variant, Protein variant, Electron transfer

1. Introduction

Protein Disulfide Isomerase (PDI, EC.5.3.4.1, NC_005109.4) also known as Prolyl 4-Hydroxylase Beta subunit (P4HB) is a thiol oxidoreductase and molecular chaperone studied since the 1980s [1,2]. PDI is the founding enzyme of the so-called Protein Disulfide Isomerase-like (PDI-like) family [3–6]. PDI is an emerging pharmacological target [7,8] as it appears to be implicated in a variety of pathophysiological processes such as cancer [9], neurodegenerative diseases [10], blood coagulation, [11–13] and oxidative stress [14,15]. Sharing common ancestral features with thioredoxin, the structure of PDI is composed of two thioredoxin-like (TRX-like) domains with active CXXC motif sites (both CGHC) traditionally referred to as “a and a’ domains”, and two substrate-binding domains referred to as “b and b’ domains” [16]. PDI is an

endoplasmic reticulum (ER) luminal protein captured by ER-resident receptors via a C-terminal tetrapeptide retention signal (the KDEL-retention signal)[17]. Depending on the context, the biological catalytic functions of PDI are reduction, oxidation or isomerization of thiol-proteins [18–21]. Functional investigation of the structural domains of PDI has been performed in several *in vitro* [18,22–25] and *in vivo* studies [12,14,26–28].

Like many eukaryotic proteins, *Pdi* appears to display splice variants based on whole exome sequencing or computed predictions [29–31]. Nevertheless, no systematic study on the functionality (enzyme activity) of these splice variants is currently available. Their functional importance remains to be elucidated while they might have a significant impact on the design of medical treatments targeting PDI. Thus, in this study, our objective was to identify natural variants of the PDI resulting from alternative splicing in rats and to functionally characterize them to estimate their biological significance.

2. Materials and methods

2.1 Isolation of total RNA and cDNA synthesis

Total RNA was isolated from 100 mg of rat tissues (8-week-old male and female Sprague Dawley rats - n=4 for both sexes) using the Trizol® reagent (Invitrogen) and the SV Total RNA Isolation System® kit (Promega, France) according to manufacturer's recommendations. Reverse transcription was performed using the Prime Script RT reagent Kit, Perfect Real Time® (Clontech), according to the manufacturer's recommendations. One µL of total RNA at 100 ng/µL was mixed with 2 µL of Prime Script buffer, 0.5 µL of oligodT primer (50 µM), 0.5 µL random hexameric

primers (100 µM) and 0.5 µL of enzyme in a total volume of 10 µL for 15 minutes at 37 °C and 5 seconds at 85 °C. Complementary cDNA was stored for less than 10 days at -80 °C.

2.2 Identification of *Pdi* splice variants by semi-nested PCR and TOPO cloning

Amplification of rat *Pdi* (NM_012998.2) was performed using a two-step PCR procedure with a high-fidelity polymerase (Accuprime Taq DNA Polymerase System®, Thermo Fisher) (0.2 µL) in a 50 µL reaction volume composed of 10 µM of each primer (10 µM) and 5 µL of buffer II. In the first PCR step, 5 µL of total cDNA from male rat liver was amplified with primer P1 (forward) and P2 (reverse) (Figure 1, Figure 2A and Table 1). P1 and P2 primers were designed to bind to untranslated transcribed regions (UTR3' and UTR5') to amplify canonical *Pdi* mRNA but also hypothetical alternative splice *Pdi* mRNAs. After an initial denaturation (94 °C for 2 minutes),10 PCR cycles were performed (94 °C for 2 minutes, 94 °C for 30 seconds, 60 °C for 30 seconds and 68 °C for 50 seconds). Then, this first PCR product was used as a template to explore alternative splicing of PDI by amplifying either the 5' or 3' part to visualize minority variants. For the second PCR step, 1 µL of the first step PCR product was amplified using P1 and P4 primers for amplification of the 5' part, and P3 and P2 primers for amplification of the 3' part. For both parts, 30 PCR cycles were performed (94 °C for 2 minutes, 94 °C for 30 seconds, 55 °C for 30 seconds and 68 °C for 50 seconds) (Figure 1A and Table 1).

After DNA electrophoresis, the amplicons were selectively extracted and directly cloned with the Zero Blunt Topo PCR Cloning Kit (Thermo Fisher Scientific), according to the manufacturer's recommendations. Two apparent profiles were found after DNA electrophoresis (long and short splice variants according to the full size of PDI). Five

plasmids from each of the two profiles (long and short) containing splice variants of rat PDI, were sequenced by Sanger sequencing (Biofidal, France) using SP6 and T7 primers. Sequence analysis and multiple sequence alignment were performed using CLC Sequence Viewer 8.0.0. The EMBOSS Needle online software URL: https://www.ebi.ac.uk/Tools/psa/emboss_needle/, was used to determine sequence identity and similarity after pairwise sequence alignment (Needleman-Wunsch algorithm).

Table 1: List of primer sequences for nested PCR of rat *PDI*.

Primer name	Seminested PCR primer sequences (5'-3')
P1	CGCTGCCGACGTCCGAC
P2	CACCGAGGTTTTGGGTTCAGG
P3	CAAAGATTTTCGGAGGTGAAA
P4	AAGCCCTCGGCCGCTTT

2.3 Absolute quantification of splice variants by RT-qPCR

A quantitative reverse transcription PCR (RT-qPCR) was performed for relative quantification of *Pdi* variants in rats using specific primers designed to quantify spliced variants (Figure 1): splice A primers (forward and reverse) were designed to bind to the exon 6 region; splice B, C and D forward primers were designed to bind to a specific sequence from alternative splice (to the overlap of the splice area) and reverse primers to bind to the exon 2 region. The reaction mixture contained 1 µL of cDNA (2 ng), 4 µL of 5X HOT BIOAmp® EvaGreen qPCR Mix (Biofidal, France) and 15 nM of each forward and reverse primer in a final volume of 20µL. The qPCRs were performed with the MX3000P qPCR Machine (Stratagene). After an initial enzyme activation step at 95°C for 15 min, 45 PCR cycles were performed (95° for 30 seconds, 60°C for 40 seconds and 72°C for 30 seconds). Three replicates per organ per rat (n=4 for each sex) were performed.

The specificities and efficiencies of the primers under our experimental conditions were evaluated by qPCR amplicon sequencing (Biofidal, France) and the cDNA dilution method (standard curves). All efficiencies were close to 100 %. *Gapdh* amplification in all experiments was established as a quality control for cDNA. No significant differences were found in its expression and *Gapdh* amplification was used as a housekeeping gene for qPCR normalization in all rat tissues. Absolute quantification was obtained using a standard curve from serial dilution of the plasmid obtained by TOPO cloning.

A.

Primer name	qPCR primer sequences (5'-3')	Target	Amplicon size (bp)
splicA - forward	GGTGGAGTTCTATGCCCCAT	Splice variant A	176
splicA - reverse	ACTTGATTGTGGGGTAGCCA		
splicB -forward	ACATGCTGAAGAAGAGC	Splice variant B	275
splicB - reverse	AGCTGTATATTCCTTTGGGG		
splicC -forward	CATGCTGGCCCCA	Splice variant C	184
splicC- reverse	AGCTGTATATTCCTTTGGGG		
splicD -forward	GACCTGGCCCAGCAGTC	Splice variant D	190
splicD- reverse	GGTACTTGGAAAACACATCGCT		

B.

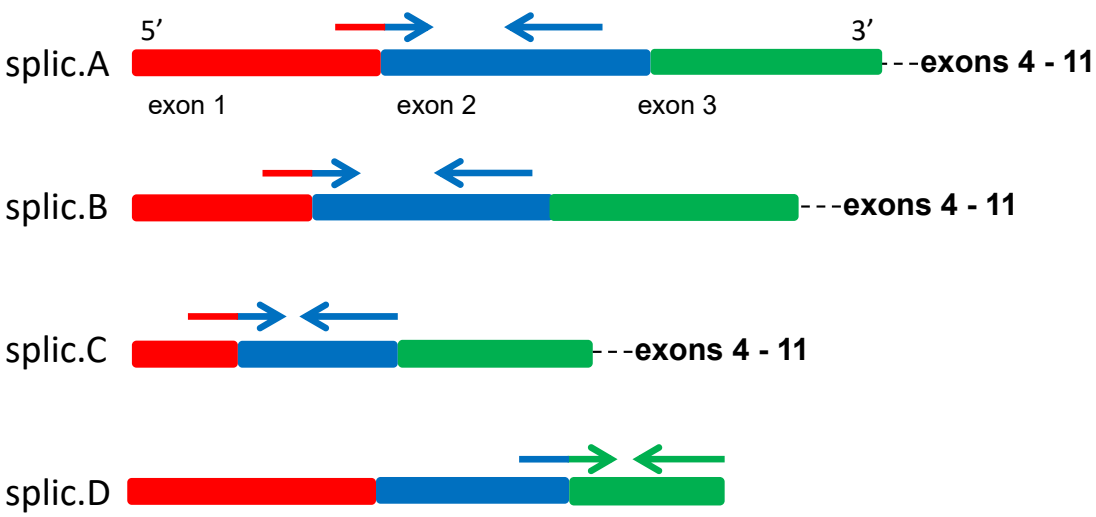

Figure 1: Primer sequences for qPCR of rat *Pdi* splice variants. (A) Table of qPCR primers used to selectively amplify rat *PDI* splice variants. (B) Selective quantification strategy. Arrow indicates the qPCR primers positions. Note that each forward primer overlaps specific the specific sequence of the considered splicing variant.

2.4 Expression and purification of recombinant PDI splice variants

Pdi splice variants were cloned into the bacterial expression vector pET-28b+ (*Bam*HI restriction site). The N-terminal hexahistidine-tagged PDI variants were expressed in Rosetta™ II (Novagen) cells grown in terrific broth medium at 37 °C and induced, when the optical density at 600 nm (OD_{600nm}) reached 0.7, by 0.250 mM Isopropyl β-d-1-thiogalactopyranoside (VWR) for 20 hours at 25 °C. After centrifugation (5000 x g for 20 minutes), bacterial spheroplasting (approximately 2.5 g of pellet) was performed in HEPES buffer (50 mM HEPES, 500 mM NaCl and 0.5 mg/L DTT) with lysozyme (0.5 mg/L) and 2 mM phenylmethylsulfonyl fluoride (PMSF), for 20 minutes at 4°C. Lysis was achieved by rapid disruption with a Potter-Elvehjem followed by sonication at 4 °C. All protein variants were purified by HisTrap™ affinity chromatography (Cytiva). Protein concentration was determined using the Pierce™ BCA protein assay kit, according to the manufacturer's recommendations.

2.5 Insulin reduction assay

The insulin turbidity test was performed according to Holmgren [32] with slight modifications. In 1 mL cuvettes, 1 µM of recombinant PDI protein was mixed in 20 mM phosphate buffer, 200 mM NaCl, 1 mM EDTA pH 7, with 16.6 mM of reduced glutathione (GSH) (Sigma Aldrich), 2 units of glutathione reductase (Sigma Aldrich, G3664), 150 µM of NADPH (VWR, PanReac AppliChem A1395). After a pre-incubation time of approximately 2 min to reduce PDI and potential traces of oxidized glutathione (GSSG), various concentrations of human insulin (Sigma Aldrich, 91077C) were added to initiate the reaction. Precipitation due to the reduction of insulin by PDI was monitored at 600 nm, and NADPH consumption at 340 nm, using a spectrophotometer UVmc² (SAFAS) at 34 °C. Rutin (PhytoLab) was dissolved in DMSO for the inhibition

experiments. NADPH was dissolved in ultra-pure water, its integrity was checked using the A_{260}/A_{340} absorbance ratio [33,34] and its concentration was measured spectrophotometrically at 340 nm using a molar extinction coefficient of 6200 $M^{-1} \cdot cm^{-1}$ at 340 nm, 25 °C in water [35,36]. The kinetics of NADPH consumption showed a lag phase. The rate was measured using the derivative of the kinetic curve at the maximum slope point, and this value was divided by the molar extinction coefficient of NADPH and the concentration of PDI to obtain a steady-state rate constant.

2.6 N,N-di(thioamido-fluoresceinyl)-cystine (DTFCys2) reduction assay

Synthesis of N,N-di(thioamido-fluoresceinyl)-cystine (DTFCys2) was performed according to the literature with slights modifications[37] : L-Cystine (12.3 mg, 0.051 mmol) and FITC (59.7 mg, 3 eq.) were dissolved in a 0.1 M aqueous solution of sodium carbonate solution (3 mL) and acetone (3 mL). The solution was stirred at 50°C for 24 hours in a sealed tube protected from light. After concentration, the crude product was purified by a column of Sephadex G-50 eluted with water affording DTFCys2 as a pure solid (20.3 mg, 39%). The 1H NMR spectrum was in accordance with the literature.

PDI splice variant reductase activities were determined using DTFCys2 as substrate. In 400 µL reaction mix, variable concentrations of recombinant PDI proteins in 20 mM phosphate buffer, NaCl 100 mM pH 7.4, were mixed with 10 µM DTFCys2 and 10 µM DTT (20 µM DTFCys2 and 20 µM DTT for Splic.B) and the increase in fluorescence due to the release of N,N-di(thioamido-fluorescéinyl)-cysteine was followed in a SAFAS Xenius fluorimeter with excitation and emission wavelengths set at 494 and 530 nm, respectively. DTT is required to allow the recycling of oxidized PDI and maintain a constant active concentration of PDI[37]. A blank was systematically recorded to account for the reduction of DTFCys2 by DTT by preincubation of 1 min

and the reaction was initiated by the addition of the PDI. The rate of the reaction in μM.s-1 was deduced by calibrating the fluorescence emission of N,N-di(thioamido-fluorescéinyl)-cysteine. The rates were linearly dependent on the PDI concentrations and the rate constant characterizing each splice variant was deduced from the slope of the rate vs. PDI concentration measured between 0.25 and 1 μM for Splic.A and Splic.C, and 1 to 5 μM Splic.B. Rutin inhibition was evaluated by measuring the rate of the reaction catalyzed by 1 μM Splic.A and 0.5 μM Splic.C.

2.7 Circular dichroism

Purified splice variants were first desalted on PD MiniTrap™ G-25 (GE Healthcare). CD spectra were recorded on a Chirascan Plus spectrometer (Applied Photophysics, Ltd, UK) with 10 μM protein desalted into sodium phosphate buffer (NaPi 10 mM, NaF 100 mM pH7.5). Quartz cells with 1 mm pathlength were filled with 200 μL of the sample, and the final result is the average of 3 independent runs. CD spectra were analyzed using the CDNN software (Boehm, 1992).

2.8 Data analysis

For gene expression analysis (absolute quantification of mRNA): the mean amount of each splice variant mRNA from each tissue (or sex) was compared to the mean of the transcripts of the others using an unpaired moderate t-test with Benjamini-Hochberg correction to minimize the false discovery rate. The Mann-Whitney U test was used to compare the apparent kinetics parameters obtained with the insulin reduction assay (apparent Michaelis constant K_M^{app} and apparent maximum rate constant k_{MAX}^{app}). P-value ≤0.05 was considered statistically significant. All statistics were performed using R software (R Development Core Team (2005). R: A language and environment for

213 statistical computing. R Foundation for Statistical Computing, Vienna, Austria. ISBN 3-
214 900051-07-0, URL: http://www.R-project.org (August 2020)).
215
216 **3. Results**
217
218 ***3.1 Pdi* presents different splice variants in rat liver**
219 The semi-nested PCR approach followed by the cloning and sequencing of the PCR
220 products revealed the expression of at least five different *Pdi* transcripts in rat liver
221 (Figure 2). The nucleotide and protein sequences of the detected splice variants are
222 summarized in Figure 2C and Figure 3, respectively. Transcript A corresponded to the
223 transcript described in the genome databases (CCDS: NM_012998.1). The other
224 transcripts (Splic.B to E) were all shorter. One of these transcripts (Splic.E) showed
225 splicing of a large portion of exon 1 including the initiation codon (from nucleotide 1 to
226 nucleotide 60) and did not exhibit alternative initiation codons. All the other splice
227 variants were coding variants. The longest coding variant exhibited a truncation of the
228 last part of the first exon (from nucleotides 8 to 94), corresponding to a loss of 29 amino
229 acids (Splic.B) (from amino acid 2 to 30). Another splice variant had a sequence loss
230 overlapping exons 1 and 2 (from nucleotides 4 to 180), corresponding to a loss of 59
231 amino acids containing the first active site of the consensus coding sequence (Splic.C)
232 (from amino acid 2 to 60 of the consensus sequence). The alignment of Splic.B, C,
233 and D with the computational predicted splice variants of P4hb in rat is shown in Figure
234 4.

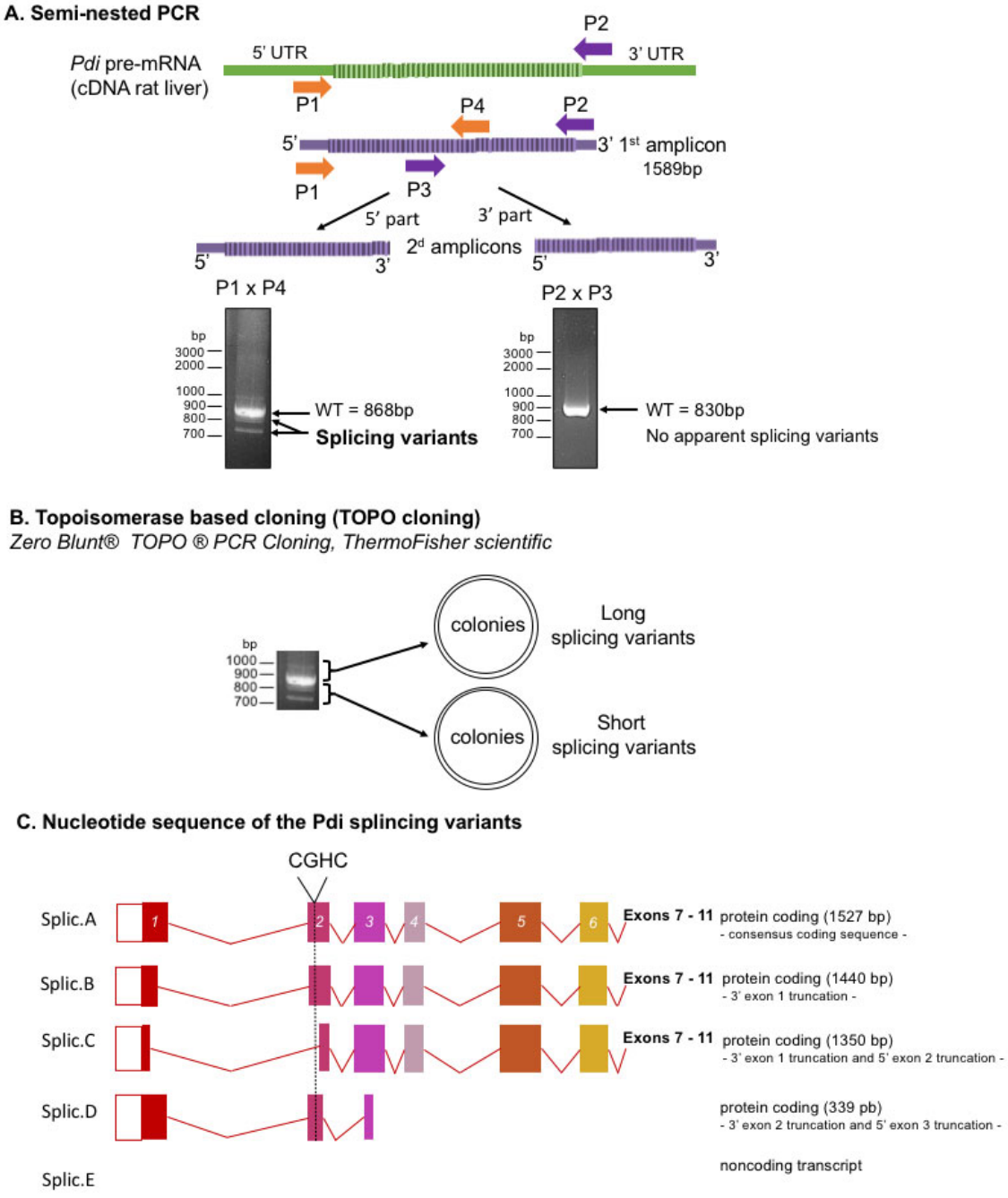

Figure 2: Major splice variants of *Pdi* in rat liver identified by the semi-nested PCR approach followed by TOPO cloning of the PCR products. (A) Semi-nested PCR strategy, P1-4: primers, WT: consensus coding sequence of *Pdi*. (B) Topoisomerase-based cloning of PCR products from P1 X P4 nested PCR. (C) Alignment of simplified splice variant structures from 5'UTR to exon 6: exons (boxes); introns (lines connecting boxes); coding sequences (filled boxes) and untranslated region (unfilled boxing).

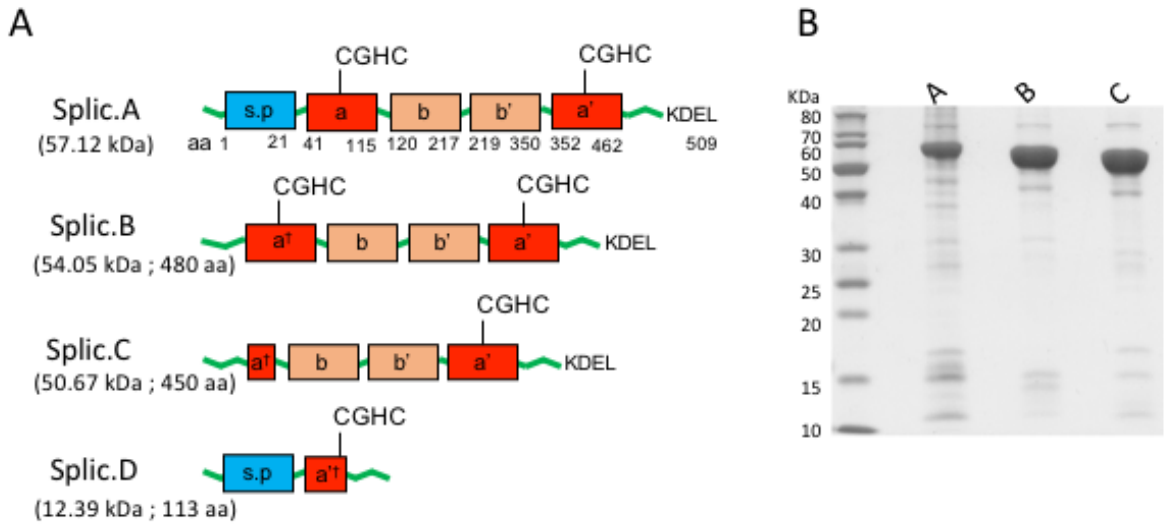

Figure 3: Protein variants of PDI. (A) Alignment of structural protein variants of PDI: catalytically active TRX-like domains (red boxes a and a'); inactive TRX domains (blue boxes b and b'); coding sequences (red boxes) and predicted signal peptide (blue box s.p); partial homology or truncated sequence compared to Splic.A (†). (B) Denaturing SDS-PAGE of His-tagged recombinant PDI protein variants expressed by *E. coli* Rosetta II cells and isolated by affinity chromatography (SDS-PAGE: 15 µg of proteins/well; colloidal aluminium-sulfate based Coomassie blue coloration, sensitivity 1 ng/band). A: Splic.A, B: Splic.B, C: Splic.C.

A

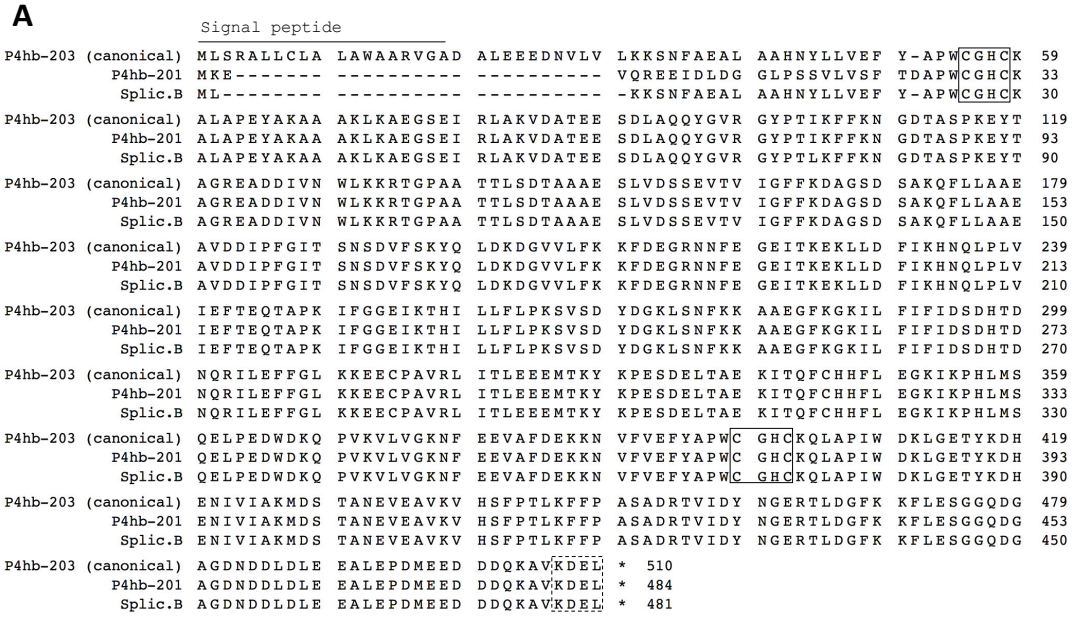
Signal peptide
P4hb-203 (canonical) MLSRALLCLA LAWAARVGAD ALEEEDNVLV LKKSNFAEAL AAHNYLLVEF Y-APWCGHCK 59
P4hb-201 MKE------- ---------- ---------- VQREEIDLDG GLPSSVLVSF TDAPWCGHCK 33
Splic.B ML-------- ---------- ---------- -KKSNFAEAL AAHNYLLVEF Y-APWCGHCK 30
P4hb-203 (canonical) ALAPEYAKAA AKLKAEGSEI RLAKVDATEE SDLAQQYGVR GYPTIKFFKN GDTASPKEYT 119
P4hb-201 ALAPEYAKAA AKLKAEGSEI RLAKVDATEE SDLAQQYGVR GYPTIKFFKN GDTASPKEYT 93
Splic.B ALAPEYAKAA AKLKAEGSEI RLAKVDATEE SDLAQQYGVR GYPTLKFFKN GDTASPKEYT 90
P4hb-203 (canonical) AGREADDIVN WLKKRTGPAA TTLSDTAAAE SLVDSSEVTV IGFFKDAGSD SAKQFLLAAE 179
P4hb-201 AGREADDIVN WLKKRTGPAA TTLSDTAAAE SLVDSSEVTV IGFFKDAGSD SAKQFLLAAE 153
Splic.B AGREADDIVN WLKKRTGPAA TTLSDTAAAE SLVDSSEVTV IGFFKDAGSD SAKQFLLAAE 150
P4hb-203 (canonical) AVDDIPFGIT SNSDVFSKYQ LDKDGVVLFK KFDEGRNNFE GEITKEKLLD FIKHNQLPLV 239
P4hb-201 AVDDIPFGIT SNSDVFSKYQ LDKDGVVLFK KFDEGRNNFE GEITKEKLLD FIKHNQLPLV 213
Splic.B AVDDIPFGIT SNSDVFSKYQ LDKDGVVLFK KFDEGRNNFE GEITKEKLLD FIKHNQLPLV 210
P4hb-203 (canonical) IEFTEQTAPK IFGGEIKTHI LLFLPKSVSD YDGKLSNFKK AAEGFKGKIL FIFIDSDHTD 299
P4hb-201 IEFTEQTAPK IFGGEIKTHI LLFLPKSVSD YDGKLSNFKK AAEGFKGKIL FIFIDSDHTD 273
Splic.B IEFTEQTAPK IFGGEIKTHI LLFLPKSVSD YDGKLSNFKK AAEGFKGKIL FIFIDSDHTD 270
P4hb-203 (canonical) NQRILEFFGL KKEECPAVRL ITLEEEMTKY KPESDELTAE KITQFCHHFL EGKIKPHLMS 359
P4hb-201 NQRILEFFGL KKEECPAVRL ITLEEEMTKY KPESDELTAE KITQFCHHFL EGKIKPHLMS 333
Splic.B NQRILEFFGL KKEECPAVRL ITLEEEMTKY KPESDELTAE KITQFCHHFL EGKIKPHLMS 330
P4hb-203 (canonical) QELPEDWDKQ PVKVLVGKNF EEVAFDEKKN VFVEFYAPWC GHCKQLAPIW DKLGETYKDH 419
P4hb-201 QELPEDWDKQ PVKVLVGKNF EEVAFDEKKN VFVEFYAPWC GHCKQLAPIW DKLGETYKDH 393
Splic.B QELPEDWDKQ PVKVLVGKNF EEVAFDEKKN VFVEFYAPWC GHCKQLAPIW DKLGETYKDH 390
P4hb-203 (canonical) ENIVIAKMDS TANEVEAVKV HSFPTLKFFP ASADRTVIDY NGERTLDGFK KFLESGGQDG 479
P4hb-201 ENIVIAKMDS TANEVEAVKV HSFPTLKFFP ASADRTVIDY NGERTLDGFK KFLESGGQDG 453
Splic.B ENIVIAKMDS TANEVEAVKV HSFPTLKFFP ASADRTVIDY NGERTLDGFK KFLESGGQDG 450
P4hb-203 (canonical) AGDNDDLDLE EALEPDMEED DDQKAVKDEL * 510
P4hb-201 AGDNDDLDLE EALEPDMEED DDQKAVKDEL * 484
Splic.B AGDNDDLDLE EALEPDMEED DDQKAVKDEL * 481

B

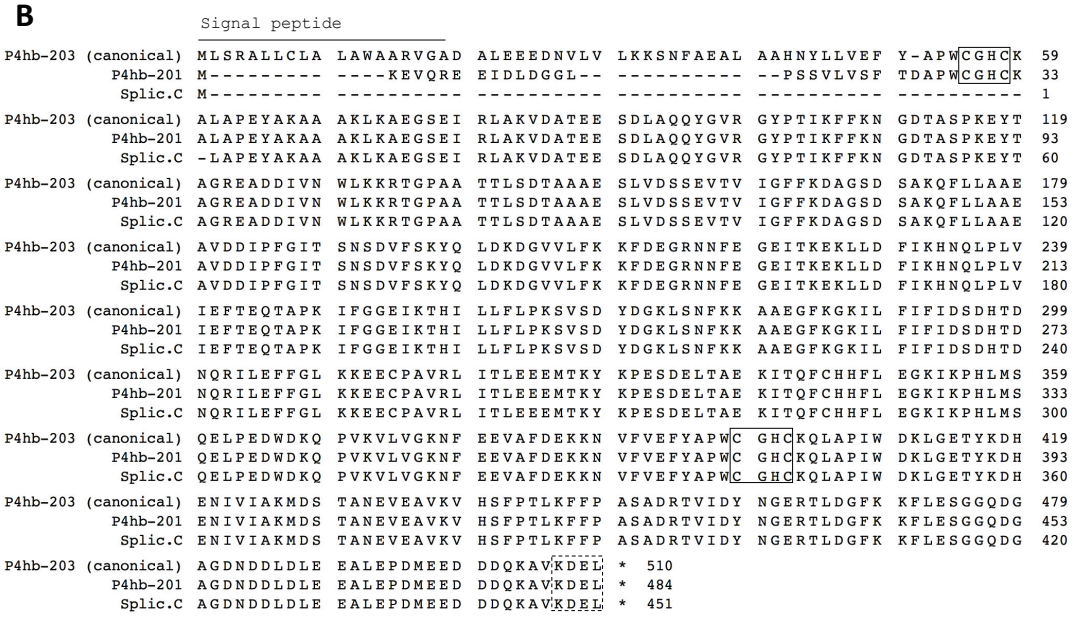
Signal peptide
P4hb-203 (canonical) MLSRALLCLA LAWAARVGAD ALEEEDNVLV LKKSNFAEAL AAHNYLLVEF Y-APWCGHCK 59
P4hb-201 M---------- ----KEVQRE EIDLDGGL-- ---------- --PSSVLVSF TDAPWCGHCK 33
Splic.C M---------- ---------- ---------- ---------- ---------- ---------- 1
P4hb-203 (canonical) ALAPEYAKAA AKLKAEGSEI RLAKVDATEE SDLAQQYGVR GYPTIKFFKN GDTASPKEYT 119
P4hb-201 ALAPEYAKAA AKLKAEGSEI RLAKVDATEE SDLAQQYGVR GYPTIKFFKN GDTASPKEYT 93
Splic.C -LAPEYAKAA AKLKAEGSEI RLAKVDATEE SDLAQQYGVR GYPTIKFFKN GDTASPKEYT 60
P4hb-203 (canonical) AGREADDIVN WLKKRTGPAA TTLSDTAAAE SLVDSSEVTV IGFFKDAGSD SAKQFLLAAE 179
P4hb-201 AGREADDIVN WLKKRTGPAA TTLSDTAAAE SLVDSSEVTV IGFFKDAGSD SAKQFLLAAE 153
Splic.C AGREADDIVN WLKKRTGPAA TTLSDTAAAE SLVDSSEVTV IGFFKDAGSD SAKQFLLAAE 120
P4hb-203 (canonical) AVDDIPFGIT SNSDVFSKYQ LDKDGVVLFK KFDEGRNNFE GEITKEKLLD FIKHNQLPLV 239
P4hb-201 AVDDIPFGIT SNSDVFSKYQ LDKDGVVLFK KFDEGRNNFE GEITKEKLLD FIKHNQLPLV 213
Splic.C AVDDIPFGIT SNSDVFSKYQ LDKDGVVLFK KFDEGRNNFE GEITKEKLLD FIKHNQLPLV 180
P4hb-203 (canonical) IEFTEQTAPK IFGGEIKTHI LLFLPKSVSD YDGKLSNFKK AAEGFKGKIL FIFIDSDHTD 299
P4hb-201 IEFTEQTAPK IFGGEIKTHI LLFLPKSVSD YDGKLSNFKK AAEGFKGKIL FIFIDSDHTD 273
Splic.C IEFTEQTAPK IFGGEIKTHI LLFLPKSVSD YDGKLSNFKK AAEGFKGKIL FIFIDSDHTD 240
P4hb-203 (canonical) NQRILEFFGL KKEECPAVRL ITLEEEMTKY KPESDELTAE KITQFCHHFL EGKIKPHLMS 359
P4hb-201 NQRILEFFGL KKEECPAVRL ITLEEEMTKY KPESDELTAE KITQFCHHFL EGKIKPHLMS 333
Splic.C NQRILEFFGL KKEECPAVRL ITLEEEMTKY KPESDELTAE KITQFCHHFL EGKIKPHLMS 300
P4hb-203 (canonical) QELPEDWDKQ PVKVLVGKNF EEVAFDEKKN VFVEFYAPWC GHCKQLAPIW DKLGETYKDH 419
P4hb-201 QELPEDWDKQ PVKVLVGKNF EEVAFDEKKN VFVEFYAPWC GHCKQLAPIW DKLGETYKDH 393
Splic.C QELPEDWDKQ PVKVLVGKNF EEVAFDEKKN VFVEFYAPWC GHCKQLAPIW DKLGETYKDH 360
P4hb-203 (canonical) ENIVIAKMDS TANEVEAVKV HSFPTLKFFP ASADRTVIDY NGERTLDGFK KFLESGGQDG 479
P4hb-201 ENIVIAKMDS TANEVEAVKV HSFPTLKFFP ASADRTVIDY NGERTLDGFK KFLESGGQDG 453
Splic.C ENIVIAKMDS TANEVEAVKV HSFPTLKFFP ASADRTVIDY NGERTLDGFK KFLESGGQDG 420
P4hb-203 (canonical) AGDNDDLDLE EALEPDMEED DDQKAVKDEL * 510
P4hb-201 AGDNDDLDLE EALEPDMEED DDQKAVKDEL * 484
Splic.C AGDNDDLDLE EALEPDMEED DDQKAVKDEL * 451

C

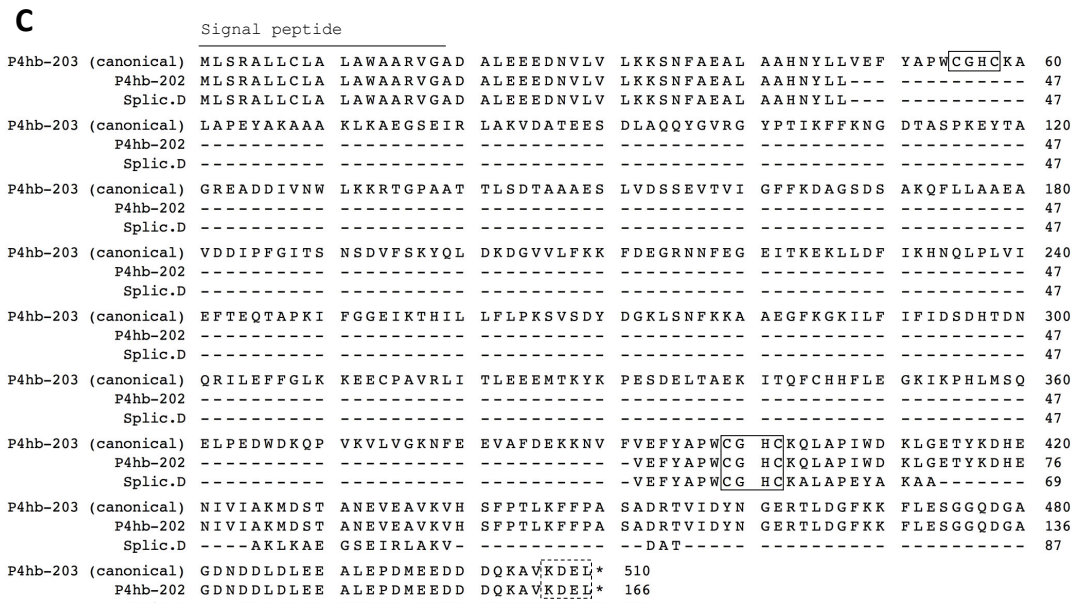
Signal peptide
P4hb-203 (canonical) MLSRALLCLA LAWAARVGAD ALEEEDNVLV LKKSNFAEAL AAHNYLLVEF YAPWCGHCKA 60
P4hb-202 MLSRALLCLA LAWAARVGAD ALEEEDNVLV LKKSNFAEAL AAHNYLL--- ---------- 47
Splic.D MLSRALLCLA LAWAARVGAD ALEEEDNVLV LKKSNFAEAL AAHNYLL--- ---------- 47
P4hb-203 (canonical) LAPEYAKAAA KLKAEGSEIR LAKVDATEES DLAQQYGVRG YPTIKFFKNG DTASPKEYTA 120
P4hb-202 ---------- ---------- ---------- ---------- ---------- ---------- 47
Splic.D ---------- ---------- ---------- ---------- ---------- ---------- 47
P4hb-203 (canonical) GREADDIVNW LKKRTGPAAT TLSDTAAAES LVDSSEVTVI GFFKDAGSDS AKQFLLAAEA 180
P4hb-202 ---------- ---------- ---------- ---------- ---------- ---------- 47
Splic.D ---------- ---------- ---------- ---------- ---------- ---------- 47
P4hb-203 (canonical) VDDIPFGITS NSDVFSKYQL DKDGVVLFKK FDEGRNNFEG EITKEKLLDF IKHNQLPLVI 240
P4hb-202 ---------- ---------- ---------- ---------- ---------- ---------- 47
Splic.D ---------- ---------- ---------- ---------- ---------- ---------- 47
P4hb-203 (canonical) EFTEQTAPKI FGGEIKTHIL LFLPKSVSDY DGKLSNFKKA AEGFKGKILF IFIDSDHTDN 300
P4hb-202 ---------- ---------- ---------- ---------- ---------- ---------- 47
Splic.D ---------- ---------- ---------- ---------- ---------- ---------- 47
P4hb-203 (canonical) QRILEFFGLK KEECPAVRLI TLEEEMTKYK PESDELTAEK ITQFCHHFLE GKIKPHLMSQ 360
P4hb-202 ---------- ---------- ---------- ---------- ---------- ---------- 47
Splic.D ---------- ---------- ---------- ---------- ---------- ---------- 47
P4hb-203 (canonical) ELPEDWDKQP VKVLVGKNFE EVAFDEKKNV FVEFYAPWCG HCKQLAPIWD KLGETYKDHE 420
P4hb-202 ---------- ---------- ---------- -VEFYAPWCG HCKQLAPIWD KLGETYKDHE 76
Splic.D ---------- ---------- ---------- -VEFYAPWCG HCKALAPEYA KAA------- 69
P4hb-203 (canonical) NIVIAKMDST ANEVEAVKVH SFPTLKFFPA SADRTVIDYN GERTLDGFKK FLESGGQDGA 480
P4hb-202 NIVIAKMDST ANEVEAVKVH SFPTLKFFPA SADRTVIDYN GERTLDGFKK FLESGGQDGA 136
Splic.D ----AKLKAE GSEIRLAKV- ---------- --DAT----- ---------- ---------- 87
P4hb-203 (canonical) GDNDDLDLEE ALEPDMEEDD DQKAVKDEL* 510
P4hb-202 GDNDDLDLEE ALEPDMEEDD DQKAVKDEL* 166
Splic.D ---EESDLAQ QSQPCLTLQL QSPWWTQAK* 114

Figure 4: Protein sequence alignment of Splic.B, C and D with the canonical sequence of rat P4hb (P4hb-203) and its most similar computational predicted splice variants.: (A) Sequence alignment of Splic. B with computational predicted P4hb isoform 201 (P4hb-201: ENSRNOT00000106240.1, Ensembl databank June 2022) (B) Sequence alignment of Splic. C with computational predicted P4hb isoform 201(P4hb-201: ENSRNOT00000106240.1, Ensembl databank june 2022) (C) Sequence alignment of Splic. D with computational predicted P4hb isoform 202 (P4hb-202: ENSRNOT00000100112.1, Ensembl databank june 2022). Active site (CXXC): full lines boxes; ER-retention sequence (KDEL): dashed lines boxes.

3.2 Tissue expression of *Pdi* splice variants differs between tissues and sex in rats

The expression level of *Pdi* variants was quantified by RT-qPCR in six tissues (aorta, gastrocnemius, gonads (testicles and ovaries), kidney, liver, and lung from 8-week-old male and female rats (Figure 1). Regardless of the tissue considered, only Splic.A, B, and C were quantifiable by quantitative RT-PCR (Figure 5). Nevertheless, since Splic.A and Splic.B mRNAs together accounted for almost 100% of all *Pdi* transcripts, Splic.D mRNAs could be considered negligible in all 6 tissues regardless of gender (Table 2).

Whatever the tissue considered Splic.A mRNAs were systematically the most abundant. They were 2.5 to 5.5 times (depending on the tissue) more expressed than Splic.B mRNAs in males; they were 1.8 to 3 times more abundant in females (Table 2). With the exception of testis, Splic.B mRNAs, in proportion to total PDI mRNAs, were most highly represented in liver in males and females; they were least represented in lung in males and in kidney for females. The proportion of Splic.B mRNAs was systematically higher in female rats than in males (except for kidney). Nevertheless, the strategy to amplify Splic.A mRNAs could also amplify undetected splice variants.

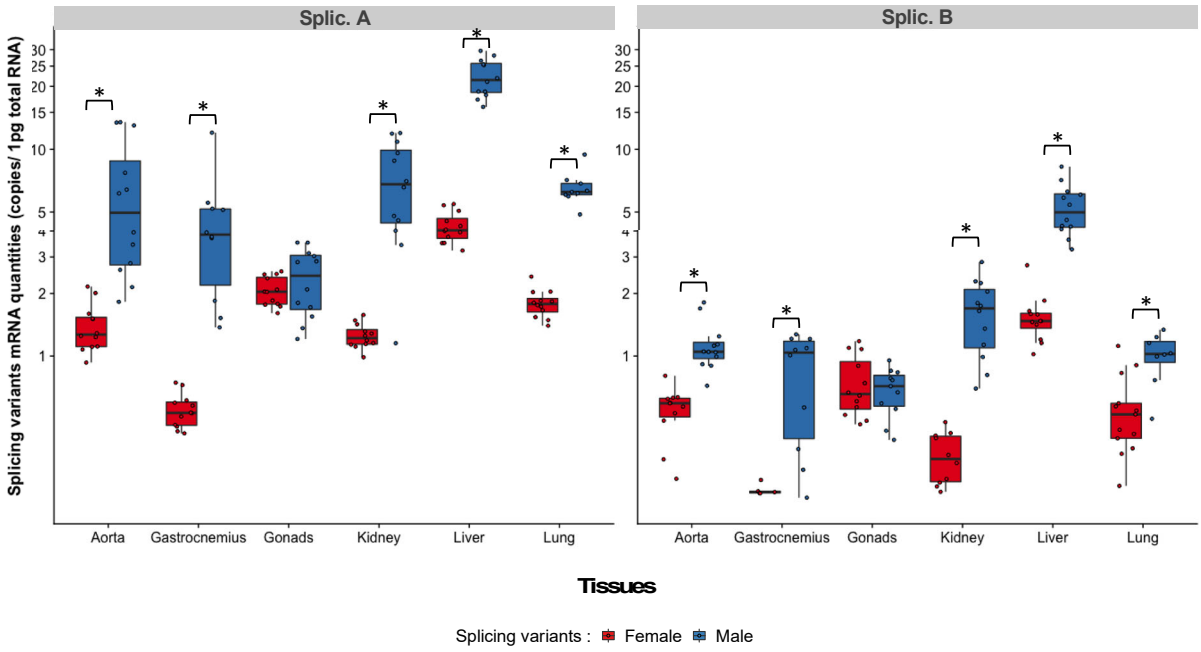

280

281 **Figure 5: Expression of *Pdi* splice variant mRNAs in different tissues of 8-week male and female**
282 **rats** (n=4 for both sexes)**.** Results are presented as number of copies/pg of total RNA. *, indicates a
283 statistically significant difference between males and females (p-value < 0.05). The Splic.C variant is
284 not shown in the figure as its quantities were too low (between 1 to 8 copies/25 ng of total RNA).
285

286 **Table 2: Proportion of RNAs of each *Pdi* splice variant to total *Pdi* transcripts in different tissues**
287 **in 8-week-old female and male rats.** Results are expressed as mean ± CI. *, significant statistical
288 difference between males and females (p value < 0.05). (p-value < 0.05).

Tissues	Splic A	Splic B	Splic C
Aorta	male: 82.1 +/- 42.2% female: 74.5 +/- 10.6%	male: 17.9 +/- 3.1%* female: 38.5 +/- 9.2%*	male: <1% female: <1%
Liver	male: 77.6 +/- 15.2% female: 67.2 +/- 9.9%	male: 22.4 +/- 4.0%* female: 36.9 +/- 6.6%*	male: <1% female: <1%
Gastrocnemius	male: 60.3 +/- 19.9% female: 71.7 +/- 10.9%	male: 16.5 +/- 6.7%* female: 31.3 +/- 7.0%*	male: <1% female: <1%
Gonad	male: 68.0 +/- 19.0% female: 74.3 +/- 5.6%	male: 28.8 +/- 4.9%* female: 36.1 +/- 7.8%*	male: <1% female: <1%
Lung	male: 83.2 +/- 8.7% female: 82.4 +/- 3.5%	male: 15.5 +/- 3.5%* female: 31.8 +/- 8.2%*	male: <1% female: <1%
Kidney	male: 76.6 +/- 31.5% female:74.2 +/- 7.8%	male: 23.4 +/- 5.9% female: 24.1 +/- 7.1%	male: <1% female: <1%

289

290 **3.3 Splic.C displays similar reductase activity to Splic.A, while Splic.B displays**
291 **lower reductase activity.**

292 Splice variants A, B, C and D were expressed as histidine-tagged proteins in E. coli
293 [38]. While Splic.A, B and C were successfully expressed and purified (Figure 3B),

Splic.D could not be expressed under the same experimental conditions suggesting instability of the corresponding protein.

The functionality of the histidine tagged Splic.A, B and C was first analyzed by their ability to reduce insulin. His-tagged-Splic.A and C proteins were shown to successfully reduce insulin in the presence of reduced glutathione. The reaction rates of Splic.A and Splic.C towards insulin followed a Michaelis-Menten model (Figure 6) allowing the determination of kinetic parameters. The apparent Km values were 56.6 ± 7.9 µM for Splic.A and 81.4 ± 7.8 µM for Splic.C, and he apparent k_{MAX}^{app} were 0.197 ± 0.007 s^{-1} for Splic.A and 0.164 ± 0.006 s^{-1} for Splic.C.

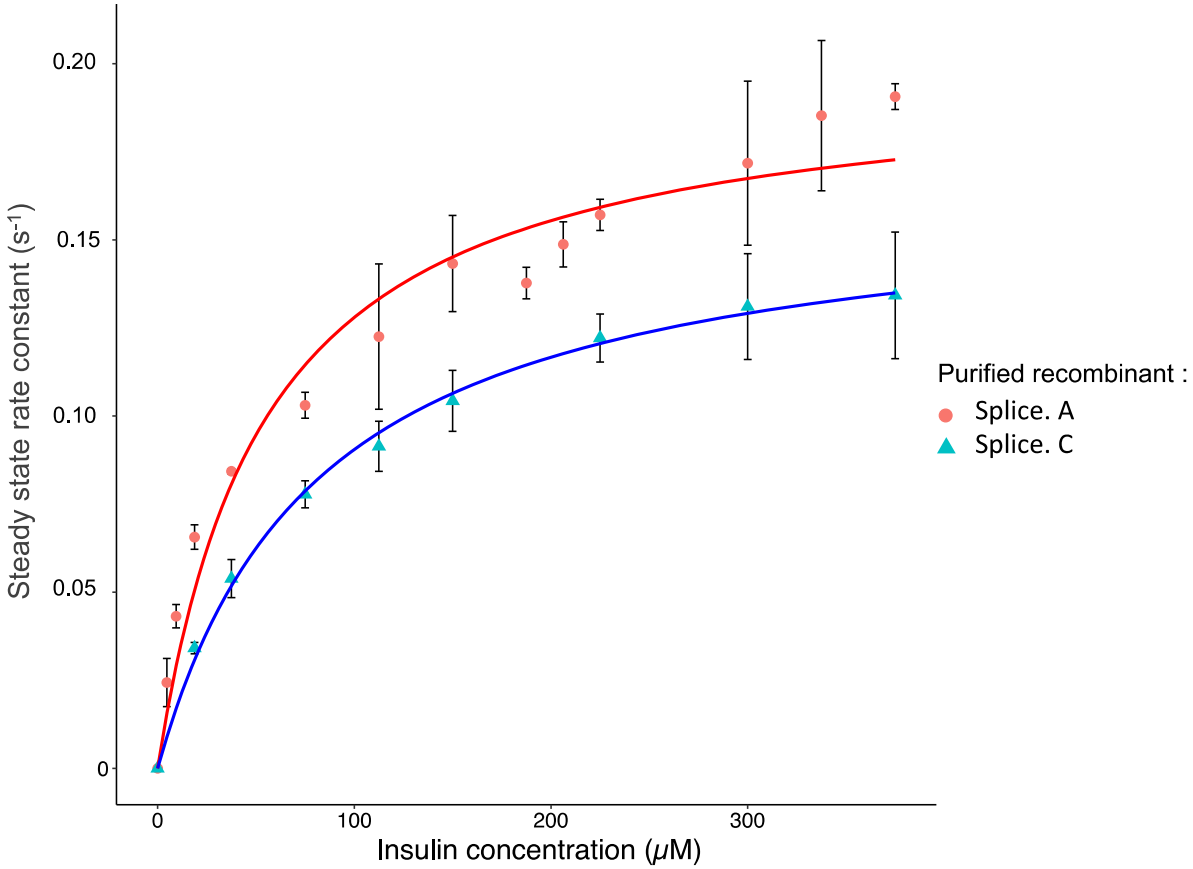

Figure 6: Insulin reduction by purified recombinant Splic.A and Splic.C as a function of insulin concentration. A (in red) and C (in blue). Measurements were done in the presence of 1 µM PDI splice variant, 16,6 mM GSH, 2 U/µL glutathione Reductase in 20 mM phosphate buffer, 200 mM NaCl, 1 mM EDTA pH 7. The reaction was initiated by adding insulin after a pre-incubation time of around 2 min. NADPH consumption was measured at 340 nm and the steady state rate constant (s^{-1}) was calculated as mentioned in Materials and Methods. Results are the mean ± SD of three independent determinations. Data were fitted by non-linear regression to the Michaelis–Menten model using R software.

No reduction of insulin by Splic.B was detected under the same experimental conditions. This absence of insulin reduction was observed with two different batches of recombinant Splic.B.

Reductase activity of splice variants was thus explored using the N,N-di(thioamido-fluoresceinyl)-cystine (DTFCys2) substrate [37]. Consistent results with those obtained with insulin were obtained using the DTFCys2 fluorescent substrate regarding Splic.A and C. These PDI variants were more active with this substrate, with reductase rate constants of 3.3 and 6.8 s^{-1} for Splic.A and Splic.C, respectively. In contrast, using the DTFCys2 substrate, reductase activity of SPlic.B was detected. This activity was 30 to 50-fold lower than that of Splic.A and Splic.C, with a rate constant of 0.12 ± 0.01 s^{-1}.

3.4 The reductase activity of Splic.B is low although its conformation is similar to that of Splic.A and B.

Because Splic.B presented low reductase activity compared to SPlic.A and C while its sequence was similar to theirs, the conformation of this variant was analyzed by circular dichroism and compared to the results obtained for Splic.A and C (Figure 7).

A

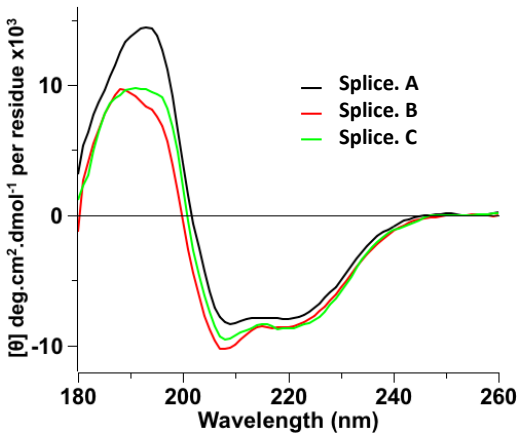

B

	Splice. A	Splice. B	Splic. C
Helix	29.70%	27.80%	28.40%
Beta-Sheet	21.20%	26.00%	24.00%
Beta-Turn	17.60%	18.80%	18.30%
Random Coil	34.60%	31.50%	33.20%
Total Sum	103.10%	104.00%	103.90%

Figure 7: Conformation analysis by circular dichroism. A/ Superimposed circular dichroism spectra of Splic.A, B, and C were determined at 10 µM of each protein. CD spectral range 180-260 nm, temperature: 20°C, step size: 1nm, bandwidth: 1nm; B/ fractions of the secondary structure components drawn from the spectra with CDNN software.

No significant differences in spectra were noticed between the three splice variants (Figure 7A), although Splic.A appeared to be the most structured protein with a stronger peak at 192 nm. Alpha helix secondary structures were present for all splice variants and accounted for nearly 30% of the signal (Figure 7B). However, a higher proportion of beta sheets was observed for Splic.B compared to Splic.A and to a lesser extent Splic.C.

3.5 Rutin similarly inhibits reductase activities catalyzed by Splic.A and C.

Inhibition of Splic.A and Splic.C-catalyzed insulin reduction by a classical inhibitor used in PDI studies, i.e. rutin (quercetin 3-rutinoside) was analyzed. For this purpose, the precipitation of insulin due to the reduction of disulfide bonds by PDI variants was measured at 600 nm [38] in the presence of 100µM of rutin as described by Lin et al. [39]. Absorbance threshold of 0.003 was considered a significant threshold for insulin precipitation. Whether the reaction was catalyzed by Splic.A or Splic.C, the reduction of insulin (Figure 8) was inhibited by the addition of rutin. The inhibitory efficacy of 100 µM rutin on Splic.C was similar to that observed for Splic.A (i.e., 94% of that observed for Splic.A). Similar results were obtained using the fluorescent DTFCys2-based assay. Rutin inhibited Splic.A and Splic.C activities by 13 and 25% at 50 µM, and by 68 and 76% at 200 µM, respectively.

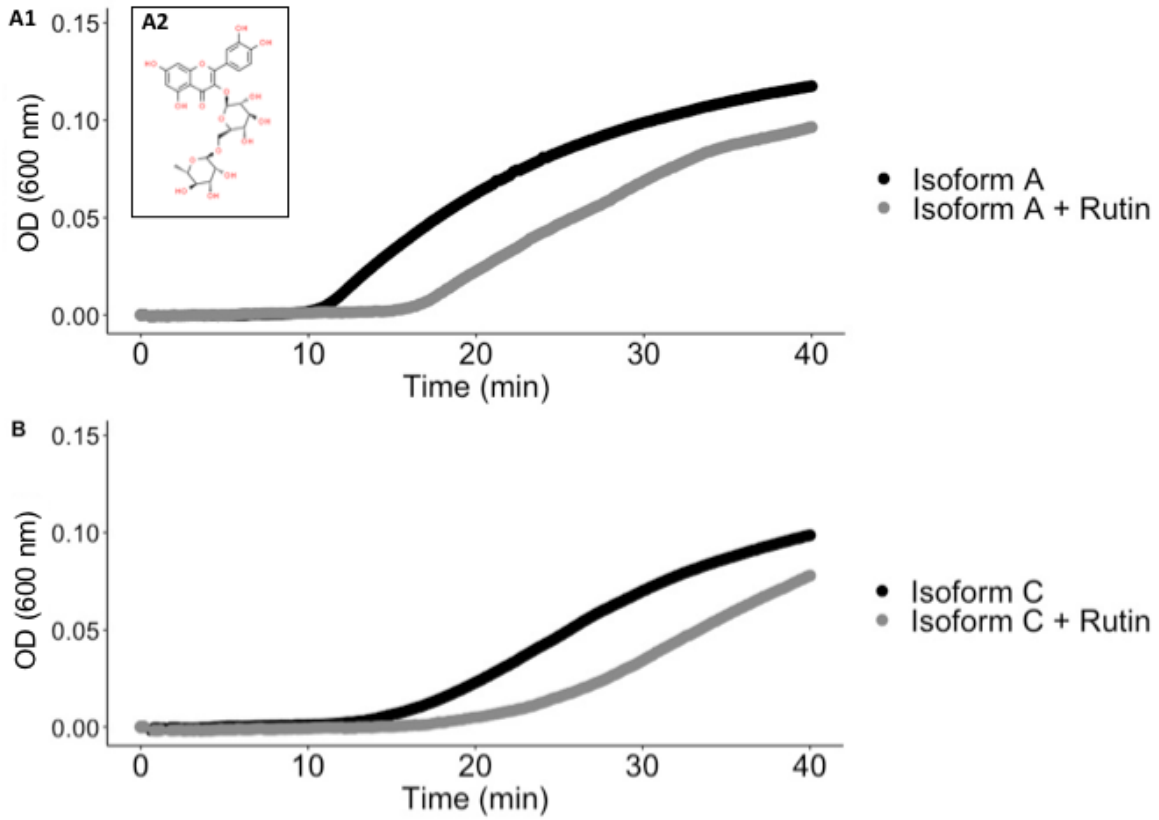

Figure 8: Inhibition of insulin reductase activity catalyzed by recombinant Pdi splice variants by rutin. The measurements were done in the presence of 1 µM PDI variant, 16,6 mM GSH, 2 U/µL glutathione reductase in 20 mM phosphate buffer, 200 mM NaCl, 1 mM EDTA pH 7, with or without 100 µM Rutin (structure in the box) and the reaction was initiated by adding 37.5 µM of insulin after a pre-incubation time of around 2 min. Insulin precipitation was monitored at 600 nm for at least 40 minutes. A/ Effect of rutin on Splic.A, B/ Effect of rutin on Splic.C.

4. Discussion

Alternative splicing of pre-mRNA is an important component of gene expression regulation and increases the complexity of the proteome. Numerous studies have proven the fundamental role of alternative splicing, for example, on proteins sub-cellular localization or enzymatic properties [29,40]. PDI is a thiol and chaperone oxidoreductase of the thioredoxin superfamily and displays multiple biological functions. Therefore, the study of PDI alternative splicing is particularly relevant. In humans, the splice variant landscape of the PDI has been described [31], and would produce 17 coding proteins (Ensembl database, *P4hb*: ENSG00000185624 - June 2022). In rats, a traditional laboratory animal used in pharmacological studies, while

three variants were computationally predicted (Ensembl database, P4hb-203 (2411 bp, 509 a): ENSRNOT00000054958.3; P4hb-201 (3123 bp, 482 aa): ENSRNOT00000106240.1; P4hb-202 (1331 bp, 165 aa): ENSRNOT00000100112.1 - June 2022), our experimental study allows to describe four coding transcripts (Splic.A, B, C and D) and one noncoding transcript (Splic. E). Alignment of their sequence with computational predictions from the Ensembl data bank (Figure 4) indicated that Splic.A matches the consensus sequence of rat PDI (P4hb-203) (100% identity and homology). Splic.B presents 93.5% identity and similarity regarding P4hb-201 and three amino acids less than P4hb-201; Splic.C, 93.0% identity and similarity regarding P4hb-201 and 33 amino acids less than P4hb-201; Splic.D, 41.6% identity and 44.9% similarity regarding P4hb-202 and 53 amino acids less than P4hb-202. Therefore, the computational predictions in rat are close to our findings for Splic.B and C. Our results are also consistent with the RNA-seq data analysis and computational predictions of *Pdi* splice variants in humans [31] (Ensembl database, *P4hb*: ENSG00000185624 - June 2022) and mice (Ensembl database, *P4hb*: ENSMUSG00000025130 - June 2022), because, in both cases, N-terminal splice variants were predominant.

PDI has been reported to be highly concentrated in the lumen of the endoplasmic reticulum and partially exported out of the cell or slightly anchored in the plasma membrane [28,41]. A part of the first exon of the canonical PDI (from aa 1 to 21) corresponds to the signal peptide contributing to the topological and subcellular localization of the protein, especially in the ER [42]). In addition to this signal peptide, PDI presents a C-terminal KDEL retention sequence in the ER inducing its retrograde transport from the Golgi to the ER, and sometimes its excretion to the cell membrane [17]. In our results both Splic.B and Splic.C show no signal peptide and lose some

amino acids from the "*a"* domain (11 amino acids for Splic.B; 41 amino acids for Splic.C) compared to the canonical PDI. On the contrary, Splic.D contains a signal peptide but does not have an ER KDEL-retention sequence. Hence, all of these splice variants could display a different cellular localization compared to PDI canonical isoform.

Despite its truncation, Splic.C is a functional splice variant. This result obtained using two different methods is not surprising considering previous work on the characterization of isolated PDI domains[39]. In fact, Splic. C is comparable to the bb'xa' fragment truncated from amino acids 2 to 60, i.e. a significant portion of the *a* domain (thioredoxin-like domain) containing the first CXXC catalytic motif[39]. The bb'xa' fragment was shown to display the same reductase activity as the canonical isoform (abb'xa'c)[39]. This is also the case of Splic.C which presents similar reductase activity than Splic.A. As expected, our results demonstrate that the loss of part of the a domain of PDI does not alter the ability of the enzyme to reduce insulin. This reduction is therefore totally mediated by the second thioredoxin-like *a'* domain (containing the second CXXC catalytic motif). Our results also confirm that the *a* and *a'* domains can function independently [18,43]. Furthermore, we show that insulin binding by Splic.C is not altered by the truncation of 59 amino acids because the apparent Km of Splic.C towards insulin is similar to that of Splic.A. This is also consistent with the literature where the b and b' domains have been described to be involved in PDI substrate binding [23,39,44] and modulation of catalytic activity [25], since the b and b' domains are conserved in Splic.C. In contrast, it was surprising to observe that, even if Splic.B contains both active sites of canonical PDI, it shows low reductase activity. Using circular dichroism, we explore the hypothesis that the

conformation of Splic.B impacts its reductase activity. Unfortunately, the slight differences observed between variants do not explain the low activity of Splic.B. Further structural studies will be necessary. The last splice variant, the Splic.D, is a short isoform presenting a partial splicing of exon 2 and 3, resulting in a premature stop codon (at amino acid 95) and a loss of the second catalytic domains (compared to canonical isoform). Based on the literature, we can hypothesize that Splic.D could act as a free thiol exchanger. Indeed, it consists of an isolated “a” PDI fragment, which has been found active in previous *in-vitro* studies [25,39]. However, due to the absence of the b' domain described as involved in substrate recognition[45], it would then act as a free thiol exchanger without substrate specificity. Similarly, it cannot be involved in the interaction with Ero1 mediating protein folding[46], since this interaction also involves the b and b' domains[47].

As PDI inhibitors are considered as potential emerging therapeutics[8,48,49], the response of splice variants to rutin, a classically used inhibitor was tested in our study. Splic.C was inhibited in the same way as Splic.A. These results are consistent with the results obtained in studies on artificial variants of PDI[39]. Indeed, the artificial variant bb'a' comparable to Splic.C was inhibited by rutin in a similar way to canonical PDI. Concerning Splic.D, only constituted by the "a" domain of PDI, and because of our inability to produce this variant, we can hypothesize that this variant is probably resistant to the action of rutin on the bases of the mechanism (rutin must interact with the "b" domain to inhibit PDI) and of the literature (the isolated "a" domain is not inhibited by rutin)[38,39]. It is therefore necessary to take into account the natural isoforms of PDI when exploring the inhibitory potential of molecules.

PDI through its multiple physiological roles interacts with many proteins, i.e., proteins involved in blood coagulation [8,41,50,51], hemostasis [12], vascular inflammation [11], infection control [52], vitamin K metabolism [53], oxidative stress [54]. The activities of Splic.A, B and C, and even D, with respect to all these targets could therefore be different, considering the differences in activity observed using insulin reduction or DFTCys2 assays. Moreover, cellular or extracellular localization could change between splice variants as previously discussed. We report herein that expression of splice variants changes according to tissue and according to gender with certainly a hormonal regulation. Such differences (activity, tissue, subcellular localization, gender) could be of major importance considering the involvement of PDI in various crucial physiological processes. An example, PDI has been identified on the surface of platelets or secreted by platelets. It contributes to the initiation of thrombus formation, through a mechanism that is currently misunderstood[13,41,55]. Some results suggest that PDI acts as an activator of tissue factor through the isomerization of cysteine residues 186 and 209, converting the encrypted version of tissue factor to active form [56]. The extracellular localization of PDI is central in this process, but little is known about the mechanism leading to this extra-ER localization. As mentioned in the literature, alternative splicing might be an explanation [51]. As it has already been demonstrated that the KDEL ER-retention signal sequence is preserved on cell-secreted PDI [57], our study leads us to question the effect of signal peptide loss on the subcellular localization of PDI. *In-vitro* and *in-vivo* models have been used to explore the role of PDI and should also be used to explore the biological functions of PDI splice variants.

In this study the distribution of splice variants according to sex and tissue was analyzed only by RT-qPCR. We attempted to do so also by western blot analysis (data not shown) using an antibody targeting the C-terminal part of the human protein claimed to cross-react with the rat protein (Proteintech, PDI Antibody 11245-1-AP). Unfortunately, we could only detect Splic.A very weakly in the liver and traces were visible in the kidney. Rat specific antibodies targeting each variant would be required to achieve better sensitivity and specificity. Nevertheless, in a recent study, western blot analysis on human colorectal tissue was performed [58] and different bands of close molecular weight were reported. It is conceivable that these different bands may correspond to splicing variants considering the differences in molecular weight observed (igure 1C in [58]). These observations highlight the need for further studies, to explore the protein expression of splice variants in rats. Tissue and sex-specific differences in the protein expression of these variants could be of major importance considering the crucial roles of PDI in many physiological processes and the possible differences in activity and localization of PDI variants.

5. Conclusion

The results of the present study show that there are different splice variants of PDI in rats. They exhibit reductase activity and could have biological relevance in protein thiol-disulfide exchange and could constitute new pharmacological targets. Indeed, only reductase activity has been explored in this study, whereas PDI also supports oxidation and isomerization reactions. Characterization of the ability of splice variants to support these enzymatic activities will be interesting, especially to assess the functional consequences of alternative splicing. Nevertheless, only a few complex methods are available to explore the isomerase and oxidase activities of PDI and are sometimes

difficult to analyze [59]. Whereas it has been described that both CXXC motifs are required for isomerase activity, does Splic.C truncated from part of the *a*-domain exhibits the same isomerase activity as canonical PDI isoform? While Splic.B supports weak reductase activity, could it have oxidase activity?

On the other hand, activation of PDI requires a protein partner, the ER oxidoreduction (Ero 1) protein. In this study, this partner was mimicked by glutathione or DTT. Functional characterization of the variants in the presence of Ero1 would be necessary, as protein-protein interactions can be modified by the different truncations. Further studies will be needed to answer to all of these questions.

Futhermore, the PDI-like family is widely conserved in all eukaryotic species from yeast to mammals [60]. Splice variants exist in other species such as humans and mice [31], the same methodology used in this study should be applied to characterize splice variants before designing pharmacological therapeutics.

Declaration of competing interest:

The authors have no competing interest to declare.

Acknowledgments:

This work was supported by a research grant from ANR (Agence Nationale de la Recherche, project ANR-18-CE20-0025).

Credit author statement:

Thomas Chetot: Conceptualization, Methodology, Validation, Formal analysis, Investigation, Writing - Original draft, Writing - Review & editing, Visualization. **Xavier Serfaty:** Methodology, Validation, Investigation, Writing - Original draft. **Léna Carret:**

Validation, Investigation. **Alexandre Kriznik**: Investigation, Writing - Original draft, Writing - Review & editing, **Sophie-Rahuel-Clermont**: Investigation, Writing - Original draft, Writing - Review & editing, **Lucie Grand**: Investigation, **Maïwenn Jacolot**: Investigation, Validation, **Florence Popowycz**: Investigation, Validation, Writing - Review & editing, **Etienne Benoit:** Conceptualization, Methodology, writing - Original draft, Project administration. **Véronique Lambert:** Conceptualization, Methodology, Writing - Original draft, Supervision, Writing - Review & editing, Project administration. **Virginie Lattard:** Conceptualization, Methodology, Formal analysis, Writing - Original draft, Writing - Review & editing, Visualization, writing - Review & editing, Resources, Supervision, Project administration, Funding acquisition.

5. References

[1] R.B. Freedman, Native disulphide bond formation in protein biosynthesis: evidence for the role of protein disulphide isomerase, Trends in Biochemical Sciences, 9 (1984) 438–441.

[2] N. Marcus, D. Shaffer, P. Farrar, M. Green, Tissue distribution of three members of the murine protein disulfide isomerase (PDI) family, Biochimica et Biophysica Acta (BBA)-Gene Structure and Expression, 1309 (1996) 253–260.

[3] C. Turano, S. Coppari, F. Altieri, A. Ferraro, Proteins of the PDI family: Unpredicted non-ER locations and functions, Journal of Cellular Physiology, 193 (2002) 154–163.

[4] F. Hatahet, L.W. Ruddock, Protein Disulfide Isomerase: A Critical Evaluation of Its Function in Disulfide Bond Formation, Antioxidants & Redox Signaling, 11 (2009) 2807–2850.

[5] J.J. Galligan, D.R. Petersen, The human protein disulfide isomerase gene family, Hum Genomics, 6 (2012) 6.

[6] D.M. Ferrari, H.D. Soling, The protein disulphide-isomerase family: unravelling a string of folds, Biochem J, 339 (1999) 1–10.

[7] H. Ali Khan, B. Mutus, Protein disulfide isomerase a multifunctional protein with multiple physiological roles, Front Chem, 2 (2014).

[8] R. Jasuja, F.H. Passam, D.R. Kennedy, S.H. Kim, L. van Hessem, L. Lin, S.R. Bowley, S.S. Joshi, J.R. Dilks, B. Furie, B.C. Furie, R. Flaumenhaft, Protein disulfide isomerase inhibitors constitute a new class of antithrombotic agents, J. Clin. Invest., 122 (2012) 2104–2113.

[9] S. Xu, S. Sankar, N. Neamati, Protein disulfide isomerase: a promising target for cancer therapy, Drug Discov. Today, 19 (2014) 222–240.

[10] T. Uehara, T. Nakamura, D. Yao, Z.-Q. Shi, Z. Gu, Y. Ma, E. Masliah, Y. Nomura, S.A. Lipton, S -Nitrosylated protein-disulphide isomerase links protein misfolding to neurodegeneration, Nature, 441 (2006) 513–517.

[11] J. Cho, Protein disulfide isomerase in thrombosis and vascular inflammation, Journal of Thrombosis and Haemostasis, 11 (2013) 2084–2091.

[12] B. Furie, R. Flaumenhaft, Thiol isomerases in thrombus formation, Circ Res, 114 (2014) 1162–1173.
[13] K. Kim, E. Hahm, J. Li, L.-M. Holbrook, P. Sasikumar, R.G. Stanley, M. Ushio-Fukai, J.M. Gibbins, J. Cho, Platelet protein disulfide isomerase is required for thrombus formation but not for hemostasis in mice, Blood, 122 (2013) 1052–1061.
[14] S. Lee, S. Min Kim, J. Dotimas, L. Li, E.P. Feener, S. Baldus, R.B. Myers, W.A. Chutkow, P. Patwari, J. Yoshioka, R.T. Lee, Thioredoxin-interacting protein regulates protein disulfide isomerases and endoplasmic reticulum stress, EMBO Mol Med, 6 (2014) 732–743.
[15] S. Lee, S.M. Kim, R.T. Lee, Thioredoxin and Thioredoxin Target Proteins: From Molecular Mechanisms to Functional Significance, Antioxid Redox Signal, 18 (2013) 1165–1207.
[16] N.J. Darby, M. van Straaten, E. Penka, R. Vincentelli, J. Kemmink, Identifying and characterizing a second structural domain of protein disulfide isomerase, FEBS Letters, 448 (1999) 167–172.
[17] A.-K. Bartels, S. Göttert, C. Desel, M. Schäfer, S. Krossa, A.J. Scheidig, J. Grötzinger, I. Lorenzen, KDEL Receptor 1 Contributes to Cell Surface Association of Protein Disulfide Isomerases, Cell Physiol Biochem, 52 (2019) 850–868.
[18] N.J. Darby, R.B. Freedman, T.E. Creighton, Dissecting the mechanism of protein disulfide isomerase: catalysis of disulfide bond formation in a model peptide, Biochemistry, 33 (1994) 7937–7947.
[19] E.A. KERSTEEN, R.T. RAINES, Catalysis of Protein Folding by Protein Disulfide Isomerase and Small-Molecule Mimics, Antioxid Redox Signal, 5 (2003) 413.
[20] E.S.J. Arnér, A. Holmgren, Measurement of Thioredoxin and Thioredoxin Reductase, in: L.G. Costa, E. Hodgson, D.A. Lawrence, D.J. Reed (Eds.), Current Protocols in Toxicology, John Wiley & Sons, Inc., Hoboken, NJ, USA, 2001.
[21] J. Lundstrom, A. Holmgren', Determination of the Reduction-Oxidation Potential of the Thioredoxin-like Domains of Protein Disulfide-Isomerase from the Equilibrium with Glutathione and Thioredoxint, (n.d.) 7.
[22] R. Xiao, A. Solovyov, H.F. Gilbert, A. Holmgren, J. Lundström-Ljung, Combinations of Protein-disulfide Isomerase Domains Show That There Is Little Correlation between Isomerase Activity and Wild-type Growth, J. Biol. Chem., 276 (2001) 27975–27980.
[23] J. Kemmink, N.J. Darby, K. Dijkstra, M. Nilges, T.E. Creighton, The folding catalyst protein disulfide isomerase is constructed of active and inactive thioredoxin modules, Current Biology, 7 (1997) 239–245.
[24] A. Raturi, B. Mutus, Characterization of redox state and reductase activity of protein disulfide isomerase under different redox environments using a sensitive fluorescent assay, Free Radical Biology and Medicine, 43 (2007) 62–70.
[25] R.H. Bekendam, P.K. Bendapudi, L. Lin, P.P. Nag, J. Pu, D.R. Kennedy, A. Feldenzer, J. Chiu, K.M. Cook, B. Furie, M. Huang, P.J. Hogg, R. Flaumenhaft, A substrate-driven allosteric switch that enhances PDI catalytic activity, Nat Commun, 7 (2016).
[26] S. Xu, Y. Liu, K. Yang, H. Wang, A. Shergalis, A. Kyani, A. Bankhead, S. Tamura, S. Yang, X. Wang, C. Wang, A. Rehemtulla, M. Ljungman, N. Neamati, Inhibition of protein disulfide isomerase in glioblastoma causes marked downregulation of DNA repair and DNA damage response genes, Theranostics, 9 (2019) 2282–2298.
[27] N. Lambert, R.B. Freedman, The latency of rat liver microsomal protein disulphide-isomerase, Biochem. J., 228 (1985) 635–645.
[28] S.R. Bowley, C. Fang, G. Merrill-Skoloff, B.C. Furie, B. Furie, Protein disulfide isomerase secretion following vascular injury initiates a regulatory pathway for thrombus formation, Nature Communications, 8 (2017) 14151.
[29] Z. Wang, C.B. Burge, Splicing regulation: From a parts list of regulatory elements to an

integrated splicing code, RNA, 14 (2008) 802–813.
[30] F.-O. Desmet, D. Hamroun, G. Collod-Béroud, M. Claustres, C. Béroud, Bioinformatics identification of splice site signals and prediction of mutation effects, (n.d.) 15.
[31] D. Kajihara, C.-C. Hon, A.N. Abdullah, J. Wosniak, A.I.S. Moretti, J.F. Poloni, D. Bonatto, K. Hashimoto, P. Carninci, F.R.M. Laurindo, Analysis of splice variants of the human protein disulfide isomerase (P4HB) gene, BMC Genomics, 21 (2020) 766.
[32] A. Holmgren, Reduction of disulfides by thioredoxin, J. Biol. Chem., 32 (1979).
[33] J.T. Wu, L.H. Wu, J.A. Knight, Stability of NADPH: Effect of Various Factors on the Kinetics of Degradation, Clinical Chemistry, 32 (1986) 314–319.
[34] A.E. Kaplan, E.R. Weiss, S.T. Byrne, N.M. El-Torkey, S.A. Margolis, Purified reduced nicotinamide adenine dinucleotide: responses to lactate dehydrogenase isozymes from three cell sources, Science, 212 (1981) 553–555.
[35] B.L. Horecker, A. Kornberg, The Extinction Coefficients of the Reduced Band of Pyridine Nucleotides, Journal of Biological Chemistry, 175 (1948) 385–390.
[36] J. Ziegenhorn, M. Senn, T. Bücher, Molar Absorptivities of β-NADH and β-NADPH, Clinical Chemistry, 22 (1976) 151–160.
[37] N. Onukwue, L. Ventimiglia, M. Potter, S. Aljoudi, B. Mutus, Simple fluorescent reagents for monitoring disulfide reductase and S-nitroso reductase activities in vitro and in live cells in culture, Methods, 168 (2019) 29–34.
[38] X. Wang, G. Xue, M. Song, P. Xu, D. Chen, C. Yuan, L. Lin, R. Flaumenhaft, J. Li, M. Huang, Molecular basis of rutin inhibition of protein disulfide isomerase (PDI) by combined in silico and experimental methods, RSC Adv., 8 (2018) 18480–18491.
[39] L. Lin, S. Gopal, A. Sharda, F. Passam, S.R. Bowley, J. Stopa, G. Xue, C. Yuan, B.C. Furie, R. Flaumenhaft, M. Huang, B. Furie, Quercetin-3-rutinoside Inhibits Protein Disulfide Isomerase by Binding to Its b′x Domain, J Biol Chem, 290 (2015) 23543–23552.
[40] Q. Liu, L. Fang, C. Wu, Alternative Splicing and Isoforms: From Mechanisms to Diseases, Genes, 13 (2022) 401.
[41] K. Jurk, J. Lahav, H. VAN Aken, M.F. Brodde, J.-R. Nofer, B.E. Kehrel, Extracellular protein disulfide isomerase regulates feedback activation of platelet thrombin generation via modulation of coagulation factor binding, J. Thromb. Haemost., 9 (2011) 2278–2290.
[42] A.M. Liaci, F. Förster, Take Me Home, Protein Roads: Structural Insights into Signal Peptide Interactions during ER Translocation, Int J Mol Sci, 22 (2021) 11871.
[43] K. Vuori, R. Myllylä, T. Pihlajaniemi, K.I. Kivirikko, Expression and site-directed mutagenesis of human protein disulfide isomerase in Escherichia coli This multifunctional polypeptide has two independently acting catalytic sites for the isomerase activity, J. Biol. Chem., 267 (1992) 7211–7214.
[44] P. Klappa, L.W. Ruddock, N.J. Darby, R.B. Freedman, The bJ domain provides the principal peptide- binding site of protein disulfide isomerase but all domains contribute to binding of misfolded proteins, The EMBO Journal, 17 (1998) 927–935.
[45] V.D. Nguyen, K. Wallis, M.J. Howard, A.M. Haapalainen, K.E.H. Salo, M.J. Saaranen, A. Sidhu, R.K. Wierenga, R.B. Freedman, L.W. Ruddock, R.A. Williamson, Alternative Conformations of the x Region of Human Protein Disulphide-Isomerase Modulate Exposure of the Substrate Binding b' Domain, Journal of Molecular Biology, 383 (2008) 1144–1155.
[46] A.M. Benham, M. van Lith, R. Sitia, I. Braakman, Ero1-PDI interactions, the response to redox flux and the implications for disulfide bond formation in the mammalian endoplasmic reticulum, Philos Trans R Soc Lond B Biol Sci, 368 (2013).
[47] L. Zhang, Y. Niu, L. Zhu, J. Fang, X. Wang, L. Wang, C. Wang, Different Interaction Modes for Protein-disulfide Isomerase (PDI) as an Efficient Regulator and a Specific Substrate of Endoplasmic Reticulum Oxidoreductin-1α (Ero1α), J Biol Chem, 289 (2014) 31188–31199.
[48] B. Xiong, V. Jha, J.-K. Min, J. Cho, Protein disulfide isomerase in cardiovascular

disease, Experimental & Molecular Medicine, 52 (2020) 390–399.
[49] N.B. Khalaf, M. Bakhiet, A new virtual screening approach for protein disulfide isomerase inhibitors reveals potential candidates for antithrombotic agents, PeerJ Inc., 2016.
[50] C. Reinhardt, M.-L. von Brühl, D. Manukyan, L. Grahl, M. Lorenz, B. Altmann, S. Dlugai, S. Hess, I. Konrad, L. Orschiedt, N. Mackman, L. Ruddock, S. Massberg, B. Engelmann, Protein disulfide isomerase acts as an injury response signal that enhances fibrin generation via tissue factor activation, J Clin Invest, 118 (2008) 1110–1122.
[51] S. Schulman, P. Bendapudi, A. Sharda, V. Chen, L. Bellido-Martin, R. Jasuja, B.C. Furie, R. Flaumenhaft, B. Furie, Extracellular Thiol Isomerases and Their Role in Thrombus Formation, Antioxidants & Redox Signaling, 24 (2016) 1.
[52] K. Reiser, K.O. François, D. Schols, T. Bergman, H. Jörnvall, J. Balzarini, A. Karlsson, M. Lundberg, Thioredoxin-1 and protein disulfide isomerase catalyze the reduction of similar disulfides in HIV gp120, Int J Biochem Cell Biol, 44 (2012) 556–562.
[53] T. Chetot, E. Benoit, V. Lambert, V. Lattard, Overexpression of protein disulfide isomerase enhances vitamin K epoxide reductase activity, Biochem Cell Biol, 100 (2022) 152–161.
[54] L. Tomanek, Proteomic responses to environmentally induced oxidative stress, Journal of Experimental Biology, 218 (2015) 1867–1879.
[55] D.W. Essex, K. Chen, M. Swiatkowska, Localization of Protein Disulfide Isomerase to the External Surface of the Platelet Plasma Membrane, Blood, 86 (1995) 2168–2173.
[56] N.I. Popescu, C. Lupu, F. Lupu, Role of PDI in regulating tissue factor: FVIIa activity, Thrombosis Research, 125 (2010) S38–S41.
[57] T. Yoshimori, T. Semba, H. Takemoto, S. Akagi, A. Yamamoto, Y. Tashiro, Protein disulfide-isomerase in rat exocrine pancreatic cells is exported from the endoplasmic reticulum despite possessing the retention signal, Journal of Biological Chemistry, 265 (1990) 15984–15990.
[58] R. Wang, Y. Shang, B. Chen, F. Xu, J. Zhang, Z. Zhang, X. Zhao, X. Wan, A. Xu, L. Wu, G. Zhao, Protein disulfide isomerase blocks the interaction of LC3II-PHB2 and promotes mTOR signaling to regulate autophagy and radio/chemo-sensitivity, Cell Death Dis, 13 (2022) 851.
[59] M.M. Watanabe, F.R.M. Laurindo, D.C. Fernandes, Methods of measuring protein disulfide isomerase activity: a critical overview, Front Chem, 2 (2014).
[60] A.G. McArthur, L.A. Knodler, J.D. Silberman, B.J. Davids, F.D. Gillin, M.L. Sogin, The evolutionary origins of eukaryotic protein disulfide isomerase domains: new evidence from the Amitochondriate protist Giardia lamblia, Mol. Biol. Evol., 18 (2001) 1455–1463.